Al-Azhar University Civil Engineering Research Magazine (CERM)
Vol. (44) No. (3) october . 2022

Numerical Investigation of Fully Unbonded Prestressed T- Beams with Different Ratio of Prestressing

Mohamed Talaat[1*], Ayman Khalil[2], Mohamed Kohail[3], Ayman Moustafa[4,]

[1] Ph.D. degree student, Structural Engineering department, Ain Shams University, Cairo, Egypt.
[2] Professor of concrete structures, Structural Engineering department, Ain Shams University, Cairo, Egypt.
[3] Associate professor, Structural Engineering department, Ain Shams University, Cairo, Egypt.
[4] Assistant professor, Structural Engineering department, Ain Shams University, Cairo, Egypt.
*Corresponding author: G18023328@eng.asu.edu.eg

الملخص العربي:

العناصر الخرسانية لاحقة الشد يتم استخدام نوعان من الكابلات كنوع من التسليح وهما اما الكابلات الغير مقيده وتكون بدون الكابلات والقطاع الخرسانى مثل الجروات او استخدام الكابلات المقيدة وتكون بوجود ماده الجراوت. وجود ماده لاحمه بين
قد تؤثر حالة الكابلات المقيدة مع وجود ماده لاحمه على أداء الانحناء والقص لأعضاء خرسانية اللاحقة الشد المختلفة . الغرض الأساسي من هذه الدراسة هو توفير مقارنة مباشرة بين السلوك الكمرات الغير مقيدة بقطاع بشكل (T) ذات التسليح الكامل بالكابلات الغير مقيده من التجارب المعملية مع نسب مختلفة فى قيم الكابلات المستخدمة فى التسليح. تم إجراء دراسة نظرية تفصيلية للعناصر المدروسة باستخدام الدراسات الغيرخطية بتقنيات النمذجة المطورة.
توجد العديد من الأساليب التحليلية والرقمية لنمذجة العناصر الخرسانية الانشائية لكن طريقة التحليل الخطى للعناصر المحدودة (FEA) هي طريقة عددية تُطبق على نطاق واسع على الهياكل الخرسانية بناءً على استخدام السلوك غير الخطي للمواد. يكمن التحدي المتمثل في نمذجة الهياكل الخرسانية سابقة الإجهاد في تمثيل العلاقة الاتصال بين الكابلات لاحقة الشد مع العنصر الخرسانى مع تمثيل الاجهاد الواقع من الكابلات نتيجة الشد على الكتلة الخرسانية. حيث تعتمد طريقة التمثيل (FEA) على تطبيق تقنية النمذجة لدراسة التأثير.
تم تصميم كمرتين بطول كامل مقدارة ٥،٠٠متر حيث ان الكمرات بقطاع بشكل (T) ذات التسليح الكامل بالكابلات الغير مقيده تم تصميمها وصبها باستخدام خرسانة ذات اجهاد طبيعى . تم اختبار الحمل على الكمرات (حتى الانهيار) تحت تأثير عزم الانحناء تم دراسة نواتج الاحمال التشغيليه واحمال الانهيار ونتائجهم النهائية ، بما في ذلك التشرخ ، وتصلب الانحناء ، وقوة الانحناء ، ومقارنتها بنتائج التمثيل النظرى بتقنية النمذجة (FEA). تم استخدام حزمة البرامج ABAQUS وتم التوصل لتوافق كبير بين النتائج المعملية ونتائج التمثيل بالنمذجة النظرية من حيث شكل تكون الشروخ بطول القطاع. وبمقارنة النواتج المعملية للانحناء فى الكمرات بالنواتج النظرية اظهرت توافق مرضى للنواتج اثناء الاختبار حتى مرحلة الانهيار على كامل طول الكمرات. كما انة تم استنتاج قيم الاجهاد فى الكابلات حتى مرحلة الانـهيار فى العينة عن طريق النمذجة.

1- Abstract:

The post-tensioned (PT) concrete member can be reinforced with either bonded or unbonded prestressing tendons. The bound condition of tendons may influence the flexural and shear performance of various PT concrete members. The primary purpose of this study is to provide a direct comparison between the experimental behavior of tested fully prestressed unbonded post-tensioned (UPT) T-beams with different ratios of prestressing steel. A detailed nonlinear finite element analyses were conducted using the developed modeling techniques.

Several analytical and numerical approaches exist for modeling concrete structural members. Finite-element analysis (FEA) is a numerical method widely applied to concrete structures based on the use of the nonlinear behavior of materials. The challenge of modeling prestressed concrete structures lies in treating the interface between concrete and prestressing tendons—the FEA-modeling technique discussed in this study is based on general-purpose finite-element packages.

Two 5.00 m length fully unbonded prestressed T-beams were designed and cast using normal strength concrete (NSC). The girders were instrumented to monitor deflection, post-tensioned losses, tendons, and concrete strains. The girders were load tested (until failure), predominantly under flexure. Their service and ultimate results, including cracking, flexural stiffness, flexural strength, were investigated and compared with FEA results. The software package ABAQUS was used to simulate these girders and their bonding conditions to verify the accuracy of FEA. An excellent agreement was achieved for numerical and experimental crack patterns. A comparison of finite element modeling (FEM) with experimental results for deflection up and down from load shows satisfactory consistency up to failure throughout the load history of the beam. Compare FEM and experimental results. Finite-element modeling overestimates stress in prestressed tendons at the ultimate state of specimens.

Keywords: Unbonded tendon; modeling; performance; post-tensioned concrete; ABAQUS; and Finite-element

2- INTRODUCTION:

Prestressed concrete is essential in many applications today to fully use concrete compressive strength and, through proper design, control cracking, and deformation. In General, prestressed concrete can be constructed in one of two ways: unbonded post-tensioned (UPT) concrete, and bonded post-tensioned (PT) concrete. Although the design methods have been developed for prestressed concrete for a long time, understanding the structural mechanism in PT concrete members still needs to be significantly enhanced in many aspects. Only a few studies have compared the behavior of PT concrete simple members with different types of tendon systems or tendon bonding conditions. It was conducted a series of PT beam tests by (Mattock, Yamazaki, Kattula, & Proceedings, 1971), it was investigated the difference in ultimate bending moment strength between bonded and non-bonded PT beams. To assess flexural strengths, (Cooke, Park, & Yong, 1981) tested 12 PT one-way slabs with bonded or unbonded tendons. These essential data are reexamined in this study as the basis to validate the proposed numerical modeling to better understanding the lack of direct experimental comparisons in the researches mentioned above, one of this paper's main focuses is to develop a reliable, general-purpose, finite-element modeling approach for unbonded PT members. With the developed numerical techniques in many other areas where experimental assessment is usually complicated, past experiments were robustly reproduced to extend and apply the modeling. Numerical assessment for the effects of tendon unbonded is carried out as the first attempt to provide the proposed modeling. The effect of tendon unbonded condition on the moment-shear interaction (that is, transfer of unbalanced moment by eccentric shear) was investigated at unbonded PT.

It was using the finite element for modeling applications to prestressed concrete have been studied for decades since the pioneering work of (Ngo & Scordelis, 1967). The key to simulating different types of prestressed systems lies in simulating the bond between tendons and the surrounding concrete. This type of numerical modeling is relatively straightforward and many researchers has been used at their studies (Kawakami, Ito, & structures, 2003; Mercan, Schultz, & Stolarski, 2010; Stavroulaki, Stavroulakis, Leftheris, & structures, 1997). In contrast, numerical simulations of bonded (before grouting) or non-bonded post-tensioned members require non-bonded formulations. Previous studies on this formulation have been carried out by a small number of research groups(El-Mezaini, Balkaya, & Çitipitio g ˇ lu, 1991; El-Mezaini & Çıtıpıtıo g ˇ lu, 1991; Kang & Scordelis, 1980; Vecchio, Gauvreau, & Liu, 2006) developed nonlinear iterative procedures to simulate non-bonded and bonded PT systems, which are limited to beam members.(El-Mezaini et al., 1991; Vecchio et al., 2006) developed the link element to study the sliding behavior of unbonded tendons.(Vecchio et al., 2006) created a formulated model for the slip behavior of fully and partially unbonded tendons in PT beams. They incorporated this into their nonlinear finite element algorithm. However, the applicability of the algorithm is limited to the two-dimensional membership case and is not available to the public. The current study used a series of numerical simulations using the (ABAQUS 2008) finite element analysis (FEA) package to simulate the structural performance of fully unbonded UPT T-Beams with different ratio of prestressing steel. A practical and accurate modeling approach was developed and applied to successfully evaluate the performance of PT members. With the help of the developed modeling techniques, it can be easy to study the following parameters and its effectiveness at the beam performance.it should refer that the change at the ratio of the prestressing reinforcement Aps cause change at the applied prestressing force f_{pe} at the section which directly effect at the hole performance of the girders. So, it should be discussed the previous studies at these points.

2.1- Effect of the Amount of Prestressing Steel on the Performance of (UPT):

The amount of prestressing steel, A_{ps}, is a factor strongly affecting the strength and deflection capacity of the beams with unbonded tendons. In the case of monolithic beams with unbonded tendons, it was found that as the area of prestressing steel increased, the ultimate strength capacity of the structure increased, but the deflection capacity decreased. In other words, the beam is less ductile with the increase in the area of the prestressing steel (Lou, Lopes, Lopes, & Materials, 2012; Lou, Lopes, & Lopes, 2016; Tanchan, 2001; Tao & Du, 1985). All the beams tested by (Tao & Du, 1985) with low values of combined reinforcement ratio were very ductile as they underwent large deflections of 90 to 120 mm at failure.

In addition, stress increments in tendons are also affected by Aps. The ultimate deflection decreases with the increase of the prestressing reinforcement ratio. (Lou et al., 2016) examined the tendon stress increment with the variation of prestressing reinforcement ratio and found that the tendon stress increment at the ultimate stage decreased almost linearly as the reinforcement ratio increased.

2.2Influence of Effective Prestress on the Performance of (UPT):

The effective prestress in the tendons, f_{pe}, is one of the main factors that strongly affect the performance of prestressed concrete beams. In the case of monolithic beams with unbonded tendons, f_{pe} was found to affect the structure's failure modes, crack patterns, and plastic rotation capacity(Tam & Pannell, 1976; Tan & Ng, 1997).

The effects of f_{pe} on the behavior of (UPT) were investigated in several studies(José Turmo, Ramos, & Aparicio, 2006; J Turmo, Ramos, & Aparicio, 2005) . The conclusions can be summarized as follows:

1- f_{pe} directly impacts the crack pattern, at which the lower the fpe, the higher the crack pattern.
2- f_{pe} shows no influence on the stiffness of the structure while cracks are closed but strongly affects the stiffness once the cracks open, i.e., the higher the fpe, the stiffer the structure.
3- The maximum deflection at failure is also affected by the prestress. The higher the f_{pe}, the greater the failure deflection.
4- The increase in f_{pe} leads to increases in the load-carrying capacity of the structure.

(J Turmo et al., 2005) also noted that a minor decrease in the prestressing level could lead to a rapid loss of structure safety. It is seen from the above review that studies have been conducted to investigate the effects of f_{pe} on the segmental beams' stiffness, crack width, strength, and deflection capacity of the structure. However, it is noted that these studies were conducted on segmental beams with unbonded tendons. Furthermore, the effects of f_{pe} on the flexural performance of segmental beams regarding failure modes, stress increment in the tendons, ultimate strength, and deflection capacity. Also, different failure modes, such as tension-controlled or compression-controlled sections, and experimental and theoretical comparison between concrete damage, also the stiffness degradation study will be addressed in this study.

3- Experimental Details:

Four-point bending flexural tests were conducted up to failure on two full scales simply supported prestressed processes, all data is presented in Table. (1).

Each prestressed concrete T-beam is longitudinally reinforced by two kinds of steel bars (i.e. common steel bars and prestressed steel strands) for tension, only common steel bars for compression zones and 10mm diameter steel bars with a center-to-center spacing of 90mm - Shear bar to center. The spacing of stirrups and the variable values of reinforcement ratios are in accordance with the provisions of (Committee, 2008). Typical dimensions, reinforcement details, and geometry of test specimens are shown in Fig. (1).

To monitor the beam's vertical deflections during the test were also measured using linear variable deflection transducer, LVDTs at different locations Fig. (1). The beams were loaded with two concentrated point loads applied simultaneously..

Table (1): Details of Tested Specimens**:**

Legend	Beam Condition	Strand Diameter (mm)	No. of Strands (mm)	CC
(G1) B1-25-0.6”	Simple	15.24	2	25
(G2) B2 -25-0.5”	Simple	12.70	2	25

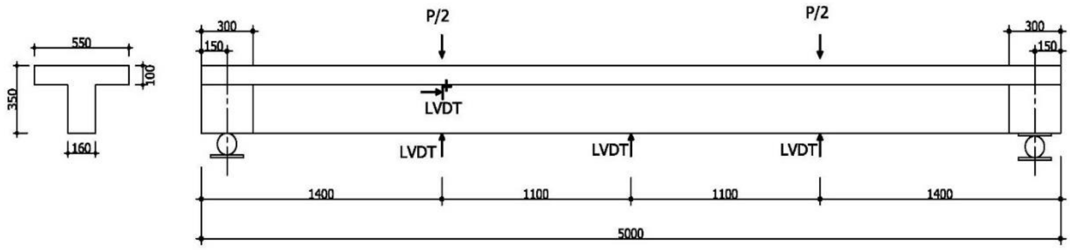

Figure (1): Details of Location of Applied Load and LVDT for (G1 – G2)

3.1- Test Setup and Instrumentation:

The beam was subjected to two concentrated loads at 1400 mm from the simple beam end edge using hydraulic jacks with 800 kN capacity. The loads were measured using a load cell of 800-kN capacity, as shown in Fig. (2).

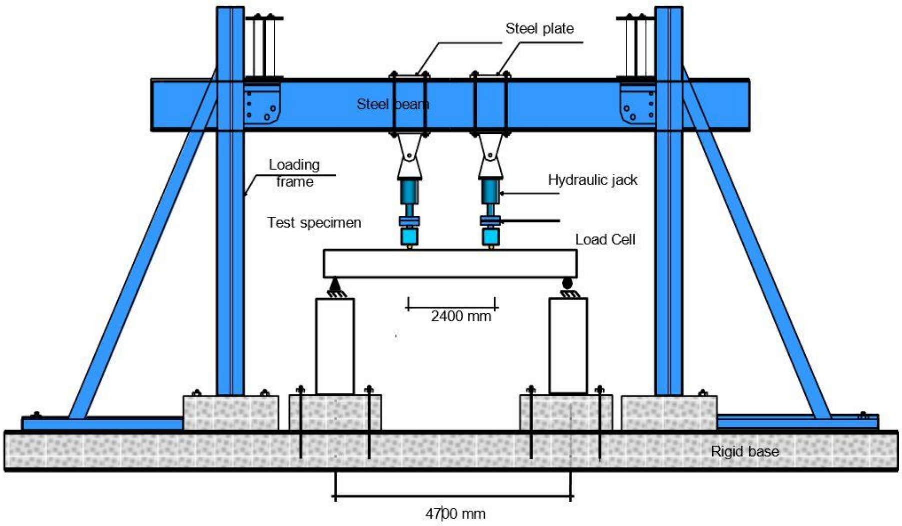

Figure (2): Test Setup for Tested Beams

4- NUMERICAL MODELING OF UNBONDED PT MEMBERS

The FEA techniques developed and described in this section for modeling the unbonded post-tensioned (PT) members, which include material assumptions, element types, and analysis procedures, with more excellent details given elsewhere (Huang, 2012)

4.1- Concrete and Steel Material Modeling:

Concrete is modeled by using the built-in “damaged plasticity model” in ABAQUS (2008). By utilizing this model, the three-dimensional stress-strain governing equations are determined from the uniaxial stress-strain relationship of concrete. The uniaxial compressive stress-strain relationship is estimated based on an existing empirical model (Carreira & Chu, 1985). The tensile relationship is assumed linear before cracking and is modeled considering tension stiffening for post-cracking behavior. The tension stiffening effect is assumed to be minor, so the stress after cracking almost linear decreases to a negligible value at approximately two times the cracking strain. An elastic-perfectly plastic model is employed for the uniaxial stress-strain behavior of non-prestressed mild steel, while a nonlinear model is used for post-tensioning tendons. The nonlinear stress-strain relationship of PT tendons is determined;(Devalupura & Tadros, 1992) developed an empirical model for Grade 270 seven-wire strands or the results obtained from the tension tests for the other types. For simplification, the nonlinear stress-strain curve is broken into piecewise linear segments. All uniaxial nominal stress-strain relations are converted into actual stress-strain relations shown in Fig. (3).

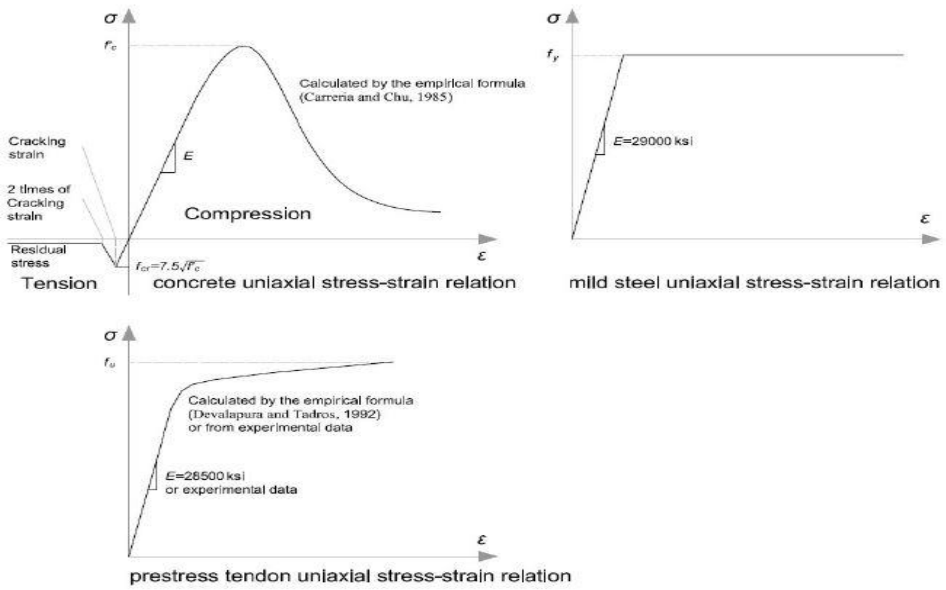

Figure (3): Finite Element Modeling Uniaxial Stress-Strain Models

4.2- Modeling Interaction Between Reinforcement and Concrete:

All non-prestressed deformed reinforcement is assumed to be perfectly bonded to concrete (that is, no bond slip is considered), as the concrete cover and spacing between reinforcing bars are almost significant in typical post-tensioned beams and slabs. Furthermore, the bond-slip effects are considered trivial because of the small bar size and amount of non-prestressed steel in typical PT members. The constraint of perfect bond is implemented in the modeling using the embedding technique. The non-prestressed deformed steel bar truss element nodes embedded in the concrete are forcibly treated to meet the displacement compatibility with the surrounding concrete brick element nodes, thereby ensuring the perfect bond between the steel bar and the concrete.

The unbonded state of prestressed tendons was modeled using previously developed spring methods (Huang, 2012; Huang, Kang, Ramseyer, Rha, & Mechanics, 2010) or contact formulations, where inequality constraints in the contact area are enforced by penalized methods, as shown in Fig. (4).

4.3- Modeling Prestressing Procedures:

To obtain finite element modeling (FEM) bending behavior of a pretensioned T-beam, the beam geometry is modeled, constrained, and meshed; non-prestressed steel and stirrups are added to the model; The bottom side is pre-tensioned with eight equal eccentric bars, and the load area is applied Fig. (5).

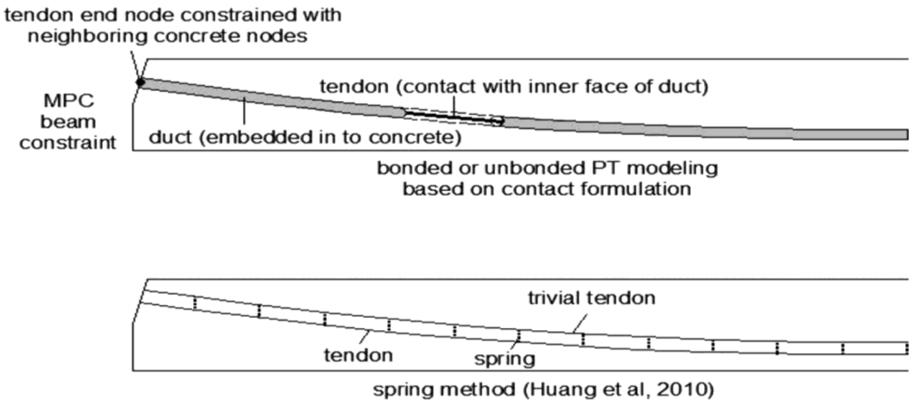

Figure (4): Modeling Details for Bonded or Unbonded PT tendons.

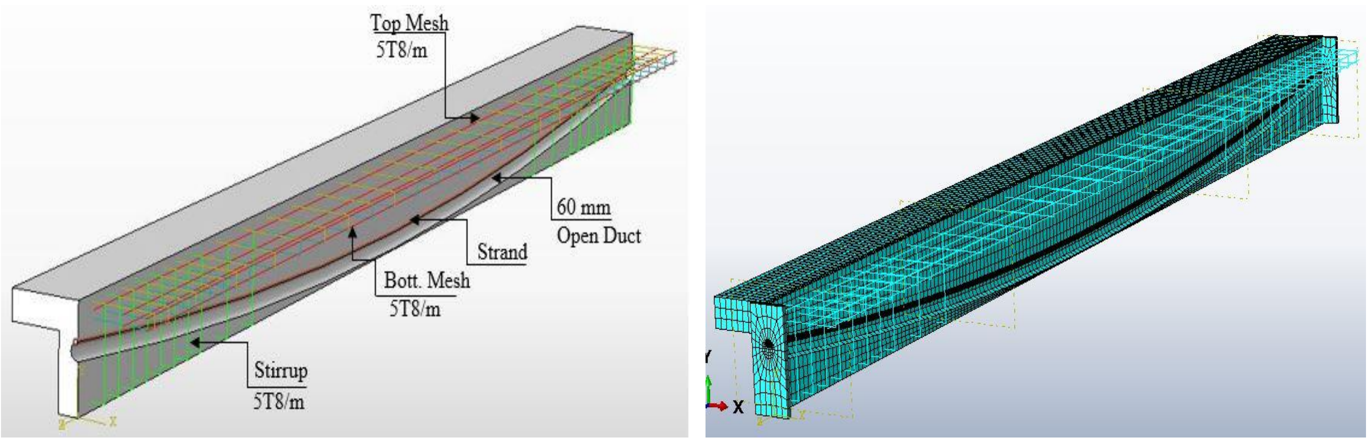

Figure (5): Typical Half Beam Detailed, Meshed with Simulated the Strand Curvature, End Anchor and Reinforcement.

5-Numerical Results and Validations:

5.1 Load–Deflection Curves Comparison:

The finite element analysis and experimental results of the upward and downward deflection of the load are shown in Fig. (6). As noted, excellent consistency was obtained throughout the load history of the beam until failure.

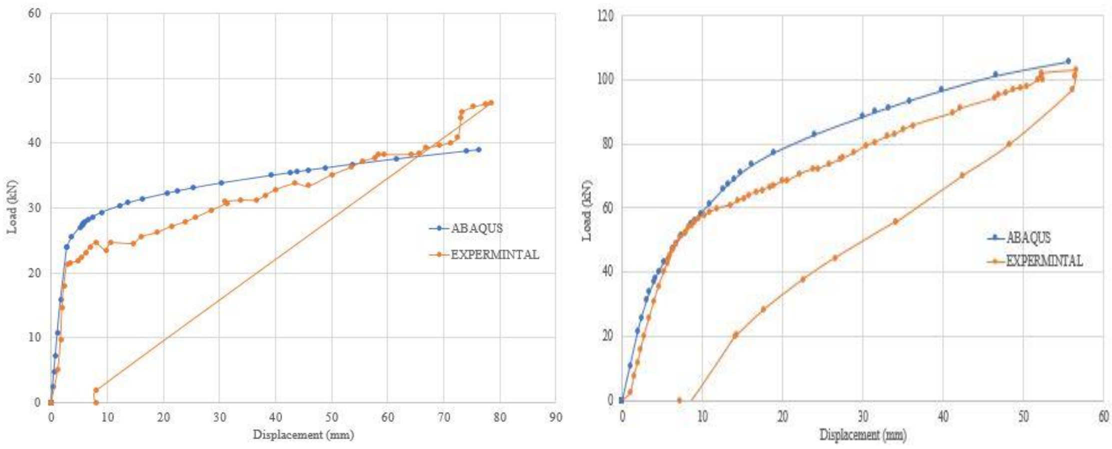

Figure (6): Comparison of Numerical and Experimental Load-Deflection Curve Specimen's G1 and G2

5.2 Effect of Amount of Prestressing Steel, A_{ps}:

Two beams with different prestressing reinforcement ratios are considered in this section in order to investigate the effect of A_{ps} on the flexural behavior of fully unbonded post-tensioning (UPT) T-beams. Both beams have the same f_{pe}/f_{pu} ratio of 0.75. Beam failure mode observed at tension-controlled at beam G2, it has more ductile cracking behavior compare with G1. The change in A_{ps} affects the load-carrying capacity and stress increment in the tendons, As observed in Fig. (7), increasing A_{ps} results in an increase in the crack load and maximum load-carrying capacity of the beam G1 also increases the stress increment in the tendon at the ultimate stage due to absence the non-prestressed reinforcement at the tension zone also the availability to slippage at the tendons due to the absence of the grout bond.

Since the stress increment in the tendon is generated by the deformation of the beam and it shows to be linearly related to the deflection of the beam, this increment in the tendon stress explains the reduction in the deflection capacity of the beam, when A_{ps} increases the strands resists all the applied loads after the concrete reached the crack point. Beam G1 deforms approximately 57 mm at the ultimate stage while those for Beam G2 are 80 mm, respectively. Similar conclusions were made from previous studies on monolithic beams with internal unbonded tendons (Lou et al., 2012; Lou et al., 2016; Tanchan, 2001; Tao & Du, 1985) as the area of pre-stressing steel increased, the ultimate strength capacity of the structure increased, and the deflection capacity decreased

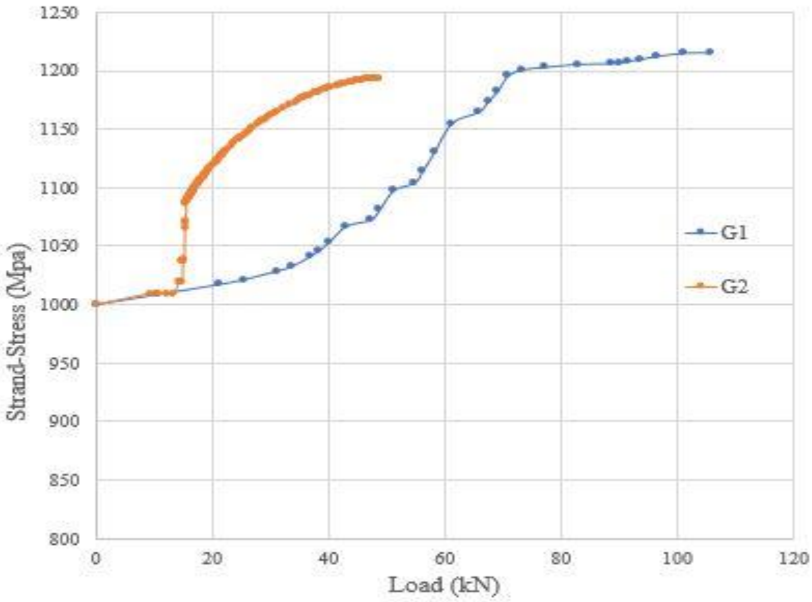

Figure (7): Comparison of FE modelling results of tendon Stress Increases Vs. Applied Load for G1 and G2

The prestressing reinforcement ratio also affects the crack distribution and the concrete stress distributions. The yield point is adopted in this study to represent the transition between the first stage of behavior when the cracks still close and the second stage when the cracks open. Two numerical models with different values of Aps are built, varies from 198 to 280.mm² which lead to increasing at the prestressing force with ratio 30% almost.

The concrete compressive stresses in the bottom fiber at the mid span, σ_c, due to f_{pe} are measured, which are in between 4.39 MPa and 29.80 MPa (σ_c/f'_c = 0.12 to 0.68), As observed in Fig. (8), It is seen from the figure that there is an almost relationship between the ratio f_{psYP}/f_{pe} and the prestressing reinforcement ratio. In other words, As observed in Fig. (8), when the prestressing reinforcement ratio increases to 40%, an increase of about 12% is observed in the tendon stress. This observation deserves attention during the analysis and design of the structure for the calculation of cracking load, which is required for the calculation of the beam's deflection. Existing design codes (ASTM Industry Handbook; Committee, 2008) recommend the use of the effective prestress f_{pe} for the calculation of the cracking load for the stress
increment in the tendon at the cracking is small.

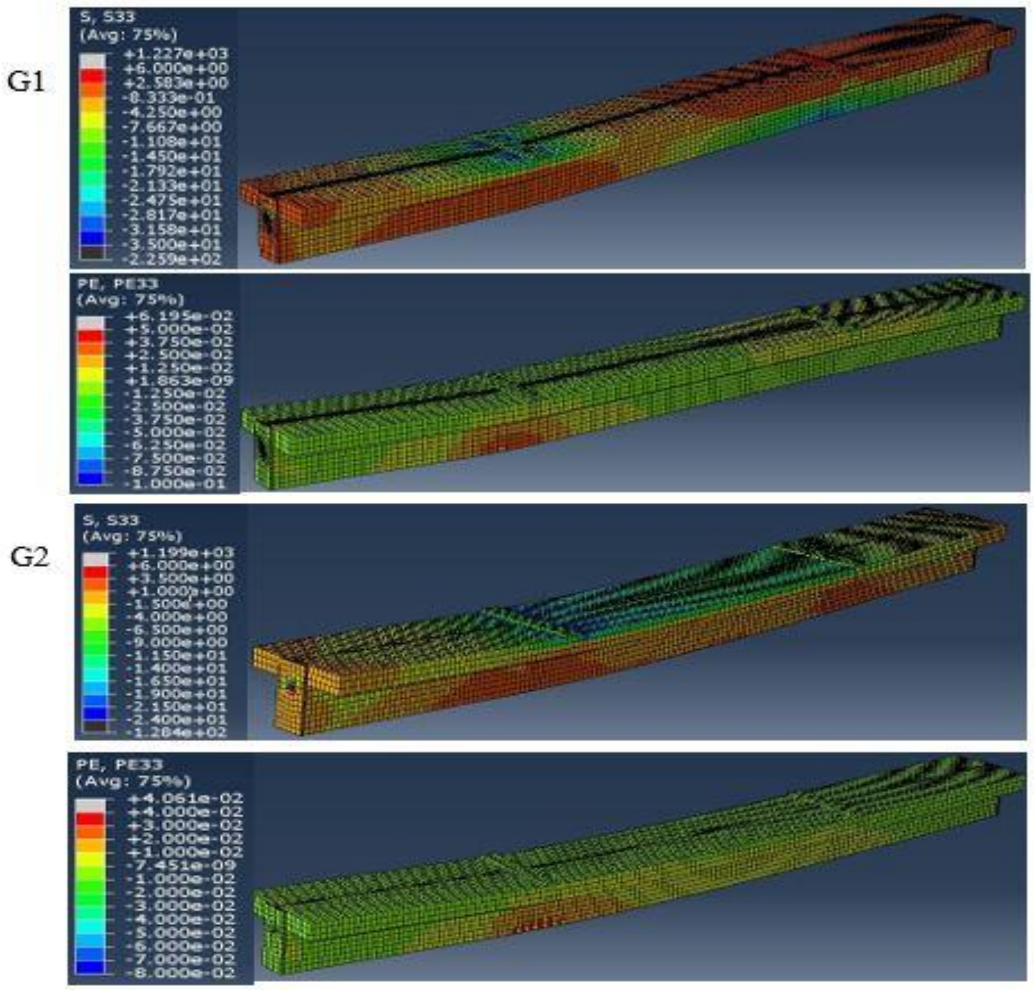

Figure (8): FE modelling Results of Concrete Stress and Strain at the Failure Loading G1 and G2

However, it can be seen from this study that the stress increment in the tendon at cracking is considerably larger than the effective prestress f_{pe} and the increment is related to the prestressing reinforcement ratio. Therefore, the increase in the tendon stress at the yield point should be taken into consideration during the calculation of the crack load in order to yield a better prediction of the beam's deflection. prestressed tendons at the ultimate state of specimens.

6. Conclusions:

- The numerical models reported in the literature developed using Abaqus software capture well the responses of the segmental concrete beams. The verified numerical models are used to conduct intensive simulations of behavior of segmental beams with different parameters for tension-controlled, compression-controlled and balanced sections. Flexural behavior of fully unbonded prestressed (UPT) T-beams with unbonded tendons in terms of failure modes, crack pattern and stress increment in the prestressing tendons are discussed.

- From the parametric study, it was found that the effective prestress in the tendons strongly affects the bearing capacity, deflection and failure mode of concrete segmental beams. Beams with higher effective prestress have greater load-carrying capacity but less deflection in the final stage. With the same prestressing amount, the change in effective prestress can lead to the change in the failure modes from compression or tension-controlled failures.

- Increasing the prestressing reinforcement ratio leads to the increase in the load-carrying capacity of the segmental beams, but decreases the beam's deflection. The stress increment in the tendon at the cracking/opening of the crack is found to be considerable in this study however it is not considered in the current design codes. 2% to 12% increase in the tendon stress at the cracking/opening is observed in this study and this stress increment is directly related to the area of prestressing steel.

7. References:

ASTM Industry Handbook, t. E. Retrieved from http://www.icivil-hu.com/Civil-team/5th/prestressed/PreStressed%20PCI%20DESIGN%20HANDBOOK_6th_Edition.pdf

Carreira, D. J., & Chu, K.-H. (1985). *Stress-strain relationship for plain concrete in compression.* Paper presented at the Journal Proceedings.

Committee, A. (2008). *Building code requirements for structural concrete (ACI 318-08) and commentary*.

Cooke, N., Park, R., & Yong, P. J. P. J. (1981). Flexural strength of prestressed concrete members with unbonded tendons. *26*(6), 52-80.

Devalupura, R. K., & Tadros, M. K. J. S. J. (1992). Critical assessment of ACI 318 Eq.(18-3) for prestressing steel stress at ultimate flexure. *89*(5), 538-554.

El-Mezaini, N., Balkaya, C., & Çitipitio g ˇ lu, E. J. J. o. S. E. (1991). Analysis of frames with nonprismatic members. *117*(6), 1573-1592.

El-Mezaini, N., & Çıtıpıtıo g ˇ lu, E. J. J. o. S. E. (1991). Finite element analysis of prestressed and reinforced concrete structures. *117*(10), 2851-2864.

Huang, Y. (2012). *Finite element method for post-tensioned prestressed concrete structures*: The University of Oklahoma.

Huang, Y., Kang, T. H., Ramseyer, C., Rha, C. J. I. J. o. T., & Mechanics, A. M. (2010). Background to multi-scale modelling of unbonded post-tensioned concrete structures. *1*(3), 219-235.

Kang, Y.-J., & Scordelis, A. C. J. J. o. t. s. d. (1980). Nonlinear analysis of prestressed concrete frames. *106*(2), 445-462.

Kawakami, M., Ito, T. J. C., & structures. (2003). Nonlinear finite element analysis of prestressed concrete members using ADINA. *81*(8-11), 727-734.

Lou, T., Lopes, S. M., Lopes, A. V. J. C., & Materials, B. (2012). Numerical analysis of behaviour of concrete beams with external FRP tendons. *35*, 970-978.

Lou, T., Lopes, S. M., & Lopes, A. V. J. C. S. (2016). Response of continuous concrete beams internally prestressed with unbonded FRP and steel tendons. *154*, 92-105.

Mattock, A., Yamazaki, J., Kattula, B. J. A. C. I. J., & Proceedings. (1971). COMPARATIVE STUDY OF PRESTRESSED CONCRETE BEAMS, WITH AND WITHOUT BOND (PART 1).

Mercan, B., Schultz, A. E., & Stolarski, H. K. J. E. S. (2010). Finite element modeling of prestressed concrete spandrel beams. *32*(9), 2804-2813.

Ngo, D., & Scordelis, A. C. (1967). *Finite element analysis of reinforced concrete beams.* Paper presented at the Journal Proceedings.

Stavroulaki, M., Stavroulakis, G., Leftheris, B. J. C., & structures. (1997). Modelling prestress restoration of buildings by general purpose structural analysis and optimization software, the optimization module of MSC/NASTRAN. *62*(1), 81-92.

Tam, A., & Pannell, F. J. M. o. C. R. (1976). The ultimate moment of resistance of unbonded partially prestressed reinforced concrete beams. *28*(97), 203-208.

Tan, K.-H., & Ng, C.-K. J. S. J. (1997). Effects of deviators and tendon configuration on behavior of externally prestressed beams. *94*(1), 13-22.

Tanchan, P. (2001). *Flexural behavior of high-strength concrete beams prestressed with unbonded tendons*: Rutgers The State University of New Jersey-New Brunswick.

Tao, X., & Du, G. J. P. J. (1985). Ultimate stress of unbonded tendons in partially prestressed concrete beams. *30*(6), 72-91.

Turmo, J., Ramos, G., & Aparicio, Á. C. J. A. M. J. (2006). Shear behavior of unbonded post-tensioned segmental beams with dry joints. *103*(3), 409.

Turmo, J., Ramos, G., & Aparicio, A. J. E. s. (2005). FEM study on the structural behaviour of segmental concrete bridges with unbonded prestressing and dry joints: Simply supported bridges. *27*(11), 1652-1661.

Vecchio, F. J., Gauvreau, P., & Liu, K. J. A. s. j. (2006). Modeling of unbonded post-tensioned concrete beams critical in shear. *103*(1), 57.